High-Speed Diagnostics For The Study Of Droplet Breakup

Alex R. Dworzanczyk[1], Nicholaus J. Parziale[1]

1: Dept. of Mechanical Engineering, Stevens Institute of Technology, United States
*Corresponding author: adworzan@stevens.edu

Keywords: Diagnostics, Holography, Fluorescence, Laser-Induced, Hypersonic, Droplet, Multiphase

ABSTRACT

In this work, we demonstrate the use of planar laser-induced fluorescence (PLIF) and back-lit shadowgraph imaging at 1.75 MHz to study the breakup of a 1-mm-diameter liquid drop in the presence of an air jet intersecting the drop's velocity vector. For the PLIF, a 447-nm laser diode is focused to form a high-intensity sheet to excite the DCM dye suspended in the ethanol droplet. For the back-lit shadowgraphy, a 685-nm fiber-coupled laser diode is used to generate a collimated beam of light to illuminate a stream of droplets as they are disrupted by a jet of air. All the complications associated with performing experiments in a ballistic range (luminosity filter, single-event triggering, standoff distance, etc.) were taken into account in this laboratory setup.

1. Introduction

Impacts with droplets or small particles at high velocity can degrade aerospace materials, reducing transparency and other desirable properties (Lapp et al., 1954; Moylan et al., 2013). The length scales of the droplets involved can be on the order of the grain size of a material, reducing the utility of a material's bulk properties for estimating the scope of this potential damage (Adler, 1982, 1999), while both the sphericity and size of a droplet can change the degree of damage in a collision (Adler, 1982). At the same time, the interaction of the shock structure around a vehicle can disrupt a droplet, potentially altering the deleterious effects of impact (Reinecke & McKay, 1969; Barber et al., 1975; Barber, 1976). Therefore, it is important to characterize the exact breakup behavior of droplets in a multiphase flow system around an aerospace structure.

To study this breakup behavior in an environment applicable to hypersonic vehicles, experiments are to be conducted at Southwest Research Institute's (SwRI) Light Gas Gun (LGG) facility. Projectiles will be accelerated to a hypersonic velocity and aimed toward a stream of spherical liquid droplets of known diameter and spacing. This work details the demonstration of two imaging techniques, planar laser-induced fluorescence (PLIF), and back-lit shadowgraphy (Danehy et al.,

2018). For both, a laser diode is synchronized to a high-speed camera to provide high-intensity illumination while the camera shutter is open.

Planar laser-induced fluorescence (PLIF) is a technique wherein a liquid solvent is doped with fluorescent material and excited with a laser. The dyed liquid, when illuminated with a laser, emits light in a narrow range of frequencies. Optical filters can be used to separate the emitted radiation from any incident and reflected light, allowing a visual recording system to only capture the liquid's behavior.

Back-lit shadowgraphy is a technique wherein a target object is placed between a camera and a light source, and the camera records the shadow of the object and any shadows cast by disturbed air around it. In this case, shadows are cast by the liquid droplets as they break up into progressively smaller droplets.

Different liquid droplet generation mechanisms were used in these experiments as the process of droplet generation was refined.

2. Liquid Droplet Generators

Three different devices were used to generate liquid droplets approximately 1 mm in diameter. All devices rely on the principle that a jet of viscous liquid will, when its surface is agitated, experience a positive feedback phenomenon whereby a small initial disturbance grows to break a droplet off from the jet. This principle was documented in experimental and computational studies by Shimasaki & Taniguchi (2011), and the equation relating the optimal separation distance λ between consecutive droplets to the properties of the liquid jet is given by

$$\lambda = \sqrt{2}\pi d_0 \sqrt{1 + \frac{3\mu_0}{\sqrt{\rho_0 \gamma d_0}}}. \tag{1}$$

Because of the incompressibility of liquids in the relevant range of pressures, the consequent droplet radius is related to the droplet spacing by

$$(1/4)\lambda d_0^2 = (4/3) r_d^3. \tag{2}$$

A theoretical optimal frequency for the initial disturbing force applied to the liquid jet is given by

$$f = u/\lambda. \tag{3}$$

The optimal frequency is a function of the diameter of the orifice from which the jet proceeds and the properties of the liquid.

One droplet generator driven by the voice coil and permanent magnet of a surplus hard disk drive (HDD) was constructed along the guidelines given by Kosch & Ashgriz (2015); this setup was used for the PLIF experiments. For a more consistent droplet quality, another device was

constructed which used an Aurasound AST-2B bass speaker to induce vibration at a specified frequency in a thin brass tube with a 0.5 mm orifice diameter. This device was based on a modified design supplied by the University of Maryland, based on work by Reinecke & McKay (1969). The DIH experiments were conducted with isopropyl alcohol as the working fluid, while the PLIF experiments used methanol and ethanol. The direct shadowgraphy experiments used distilled water. The properties of these liquids are given in Tab. 1, as are the calculated droplet diameters for each set of experiments.

Table 1. Properties of working fluids and calculated drop sizes.

Property	Isopropanol	Methanol	Ethanol	Water
Density (kg/m^3)	786	792	789	999
μ (kg/m s)	2.4e-3	5.6e-4	1.1e-3	1.0e-3
γ (mN/m)	23.00	22.70	22.10	7.20
Experimental Orifice ID (mm)	0.24	0.6	0.6	0.5
Droplet OD (mm)	0.23	1.13	1.13	0.94

3. PLIF Laser Illumination Setup

A schematic view of the laser illumination system is presented in Fig. 1. Initially, a 520-nm laser diode (ThorLabs L520G1) was specified for these experiments but was replaced with a 447 nm laser diode (Osram PLPT9-450 LA E) because of its high nominal power (3,000 mW). The beam had to first be collimated through a combination of aspheric and cylindrical lenses to produce a light sheet of the desired width and thickness (100 μm, as imaged by a beam profiler). The Phantom TMX 7510 camera triggered the laser diode driver (PicoLAS LDP V 50-100) via a DGS645 digital delay generator. The repetition rate was 1.75 MHz with a pulse duration of 30 ns, with the exposure time of the camera set to 95 ns.

A 0.6 mm hypodermic needle was attached to the HDD-derived droplet generator, generating droplets of 1.2 mm diameter. The liquid was ethanol doped with DCM at a concentration of 0.100 g/L (similar to that of a dye laser). DCM dye in an ethanol solvent was chosen because of the high power and absorption/emission spectrum (Nabavi et al., 2018). When illuminated at this wavelength, DCM emits light at 644 nm (Brackmann, U., 2000). A band-pass filter was chosen to isolate this emitted light from the incident laser light and ambient light. The filter chosen was an Edmund Optics 631 nm filter with a 21 nm full-width half-maximum (FWHM) band and a diameter of 50 mm. The laser light sheet propagates along the Z-axis, and the droplet stream falls along the Y-axis. Here, the camera is placed along the X-axis, and the air jet is along a vector 45 degrees between the Y and Z axes.

An air jet with a stagnation pressure of 12.5 psig is used to apply an airflow at a 45-degree angle to the direction of droplet fall.

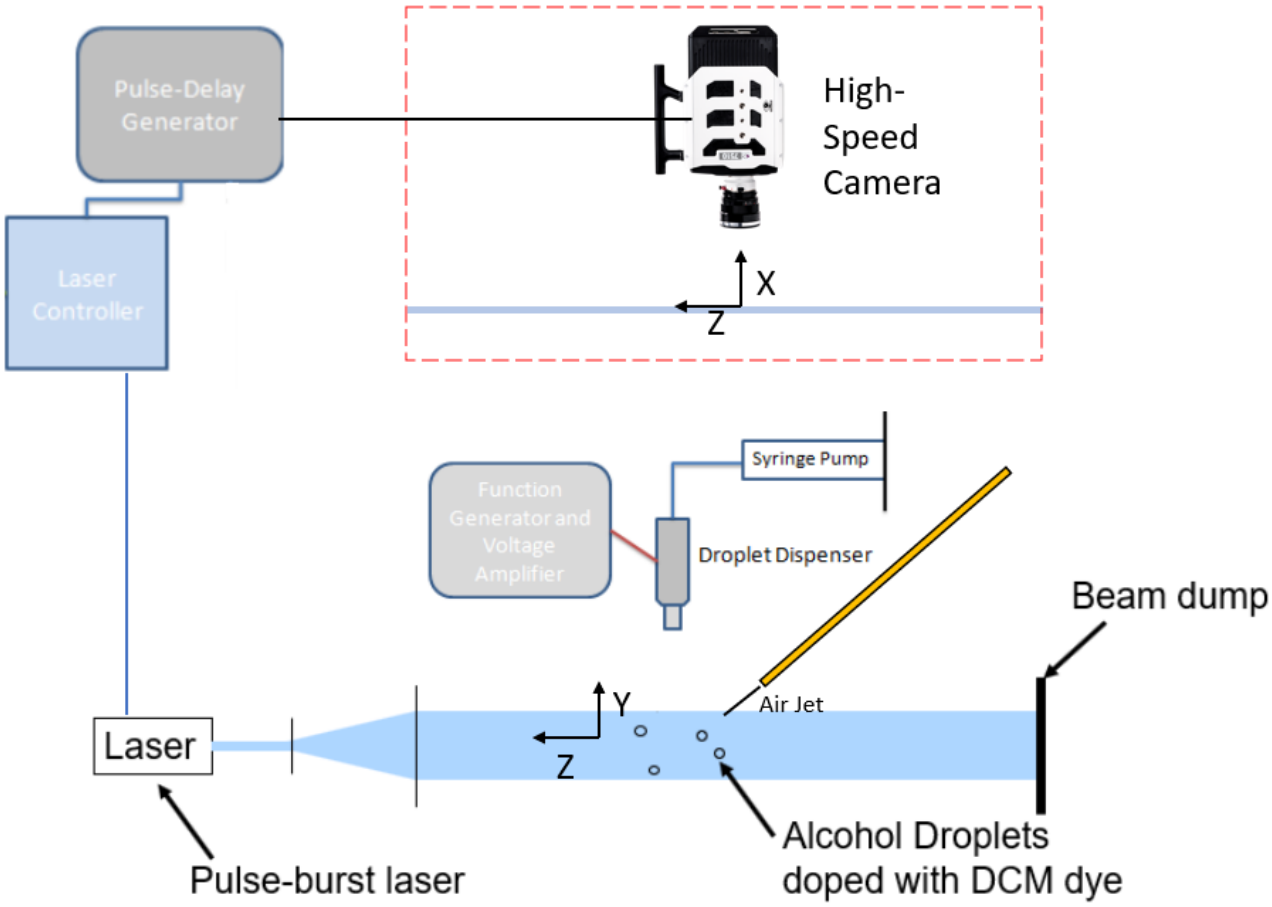

Figure 1. Planar Laser-Induced Fluorescence Illumination Schematic

4. Planar Laser-Induced Fluorescence Results

Here, we include three snapshots from two sequences of experiments. In Fig. 2 (left), we observe so-called "bag breakup," also observed by Reinecke & Waldman (1970). The bag shatters, and the liquid mass at its center dissipates and fades from view; the remaining mass of the droplet is concentrated around the former rim of the bag, now a toroidal mass of liquid. One millisecond after the initial bag breaks up, the liquid in the annulus breaks up further.

In Fig. 2 (right), noting that the experimental setup was the same, we observed what Theofanous et al. (2007) terms the "bag-and-stamen" or "umbrella" breakup regime. This is supposed to occur at slightly higher Weber numbers (~13) than the "bag" breakup regime (~7). While a "bag" of liquid still forms and inflates due to the pressure of the incident air jet, a substantial mass of liquid remains near the center of the flattened droplet face and forms a stem around which the bag inflates. The "bag" and "umbrella" breakup regimes observed by Theofanous & Li (2008) can occur at very similar Weber numbers, so the presence of both in the same experiment is not unexpected.

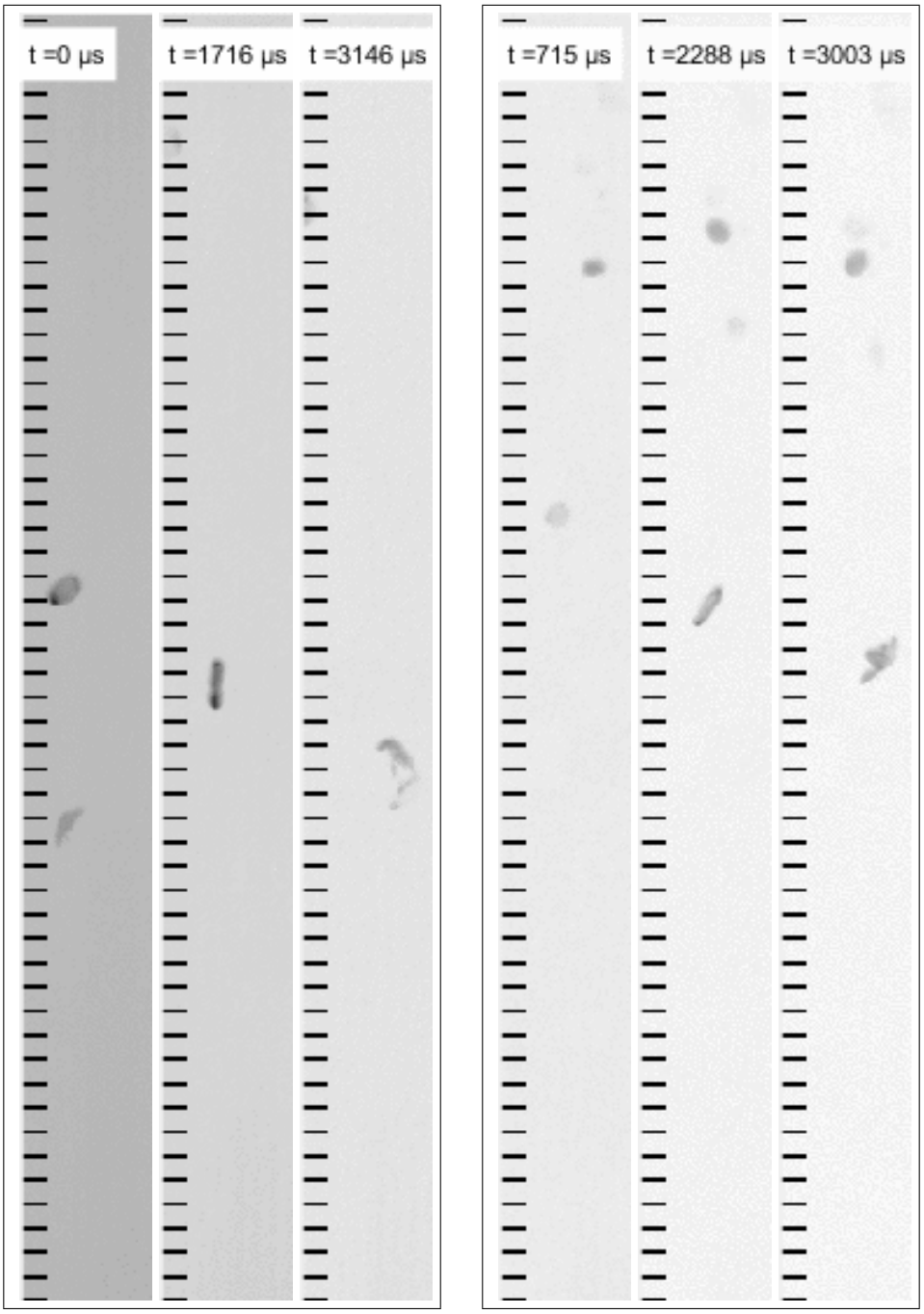

Figure 2. Left: Bag breakup of a droplet imaged at 1.75 MHz. Initially, the droplet is approximately midway up the image. Right: Umbrella breakup of a droplet imaged at 1.75 MHz. Initially, the droplet is approximately just above midway up the image. Tick marks are 1 mm. Image is not cropped.

5. Back-Lit Shadowgraphy Setup

Back-Lit Shadowgraphy is simple to implement (Settles, 2001) and provides much of the same information as more complicated arrangements like PLIF or DIH, though as Theofanous & Li (2008) notes, internal structures may be difficult to identify. The experimental setup is shown in Fig. 3. A Nikon AF Nikkor lens is used on the high-speed camera to focus the droplet to the imaging

plane. The laser diode, in this case, a 685 nm LDX Optronics LDX-3230-685 fiber-coupled diode is connected to a PicoLas LDP-V 03-100 laser controller. The output of the diode is collimated into a circular beam with a diameter of 1 inch propagating along the Z-axis. The laser controller is connected to a digital delay generator with an input from the Phantom TMX 7510 camera. The delay generator, synchronized to the camera's strobe output, generates pulses with a duration of 20 ns at the same frequency at which the camera records images (in this case, 1.75 MHz).

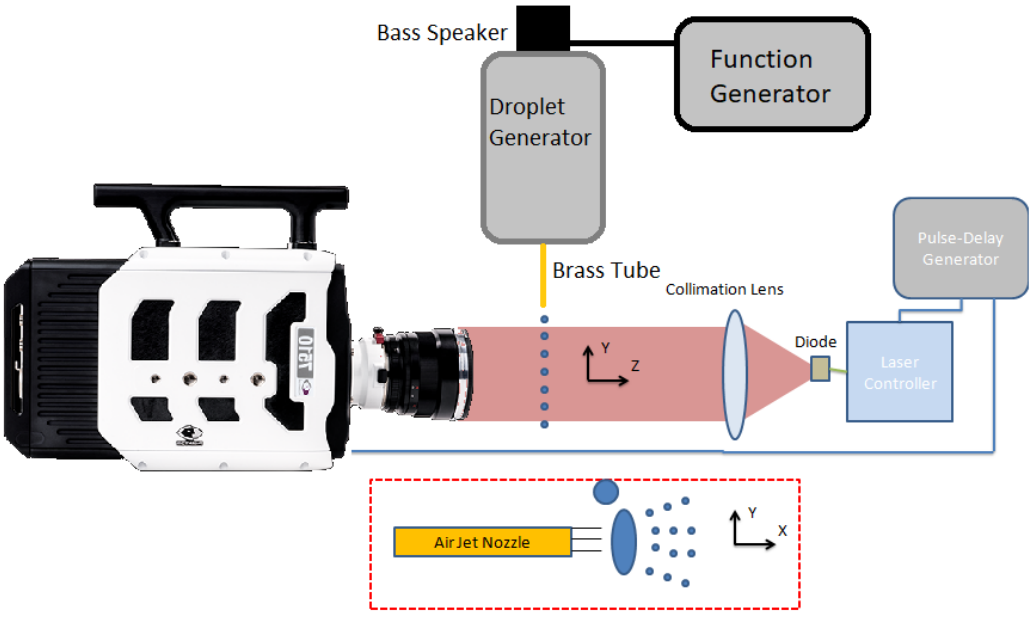

Figure 3. Shadowgraphy Illumination Schematic

6. Back-Lit Shadowgraphy Results

Before droplet breakup experiments were conducted, the camera was focused on the plane in which the droplets fell and a length scale was defined. This served also to validate the functionality of the speaker-driven droplet generator and help develop the operational technique for creating the desired liquid droplet stream. Fig. 4 shows a stream of droplets without disturbance by the air jet; the droplet diameters are consistent with the diameter calculated for water flowing through a 0.5 mm orifice.

A stream of spherical liquid droplets was generated and exposed to an air jet normal to the direction of droplet flow and to the axis of laser propagation. Still images from the videos generated of droplet breakup are presented in Fig. 5. The liquid droplet is seen to begin flattening when it enters the horizontal jet of air at 200-400 µs. Between 400-550 µs after the beginning of the recording, liquid is stripped from the windward side of the drop. Between 500-550 µs a "bag" of liquid

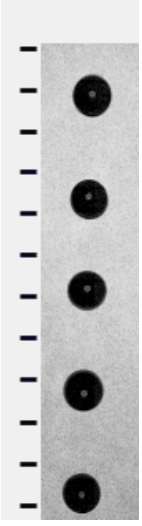

Figure 4. Stream of liquid droplets imaged at 1.75 Mfps; scale marks separated by 1 mm. Image is cropped, 25% is shown.

similar to those observed in the PLIF experiments is seen near the center of the disrupted droplet, and material continues to strip off the edges of the drop. Between 550-600 µs, the bag forms and ruptures. The droplet is completely disrupted and ejected from the gas stream at 1.082 s; some of its fragments have impacted the next droplet in the stream as it descends toward the air jet. The breakup patterns visible from 600 µs and on could be "Multi-Bag," "Multi-Wave," or "catastrophic" phenomena observed by Theofanous et al. (2007) and Reinecke & McKay (1969) at Reynolds numbers of approximately 75 in supersonic flow. While the flow in these experiments was subsonic, they were carried out at an ambient sea-level atmospheric pressure, while those of Theofanous et al. (2007) were carried out in a low-pressure tunnel. The greater atmospheric density in these experiments allows a Weber number comparable to those at which Theofanous et al. (2007) observed similar behavior. The approximate Weber number for these droplet breakup experiments was 200.

Figure 5. Back-lit shadowgraphy of droplet breakup imaged at 1.75 MHz. Tick marks are 1 mm. Image is cropped, 25% is shown.

7. Conclusions

In this paper, methods for recording 1.75 MHz holographic (reported in Dworzanczyk & Parziale (2021)), back-lit shadowgraphic, and planar laser-induced fluorescence (PLIF) images of liquid droplet breakup are described. Droplet breakup phenomena were observed matching those described in previous research. Ultimately, this study aimed to assess which of these techniques could be applied to ballistic-range experiments; such experiments have their complications, such as timing, luminosity, vibration, and importantly, the drift of the projectile off the shotline. Timing, luminosity, and vibration are tractable technical issues; however, appreciable deviation of the projectile off the shotline would complicate the interpretation of data collected with a technique with a narrow depth-of-field, which PLIF has by definition.

Acknowledgements

Dworzanczyk and Parziale were supported by ONR-MURI Grant N00014-20-1-2682 for which Dr. Eric Marineau is the program manager.

Nomenclature

γ	surface tension [N/m]
d_{drop}	drop diameter [m]
d_0	orifice diameter [m]
f	frequency [Hz]
λ	wavelength [m]
μ	viscosity [Pa s]
r	radius [m]
ρ	density [kg/m^3]
v	flow velocity [m/s]
We	Weber number

References

Adler, W. F. (1982). *Investigation of liquid drop impacts on ceramics* (ETI-CR-82-1075).

Adler, W. F. (1999). Rain impact retrospective and vision for the future. *Wear*, *233-235*, 25-38.

Barber, J. P. (1976). *Water drop breakup/impact damage thresholds* (AFML-TR-76-126).

Barber, J. P., Taylor, H. R., Grood, E. S., & Hopkins, A. K. (1975). *Water drop/bow shock interactions* (AFML-TR-75-105).

Brackmann, U. (2000). *Lambdachrome Laser Dyes* (Third ed.). Lambda-Physik AG.

Danehy, P. M., Weisberger, J., Johansen, C., Reese, D., Fahringer, T., Parziale, N. J., ... Cruden, B. A. (2018, December 3-5). Non-Intrusive Measurement Techniques for Flow Characterization of Hypersonic Wind Tunnels. In *Flow Characterization and Modeling of Hypersonic Wind Tunnels (NATO Science and Technology Organization Lecture Series STO-AVT 325).* Brussels, Belgium: NF1676L-31725 - Von Karman Institute.

Dworzanczyk, A., & Parziale, N. J. (2021, 2-6 August). High-Speed, Short-Pulse-Duration Light Source for Digital Inline Holographic Imaging of Multiphase Flow Fields. In *Proceedings of AIAA Aviation Forum 2021.* Virtual Event: AIAA-2021-2919. doi:

Kosch, S., & Ashgriz, N. (2015). A simple vibrating orifice monodisperse droplet generator using a hard drive actuator arm. *Review of Scientific Instruments*, *86*. doi:

Lapp, R. R., Stutzman, R. H., & Wahl, N. E. (1954). *A study of rain erosion in plastics and metals* (WADC 53-185).

Moylan, B., Landrum, B., & Russell, G. (2013). Investigation of the physical phenomena associated with rain impacts on supersonic and hypersonic flight vehicles. *Procedia Engineering*, *58*, 223-231. doi:

Nabavi, S. H., Khodabandeh, M. H., Golbabaee, M., & Moshaii, A. (2018). Absorption of DCM Dye in Ethanol: Experimental and Time Dependent Density Functional Study. *International Journal of Optics and Photonics*, *12*(1), 43-56. doi:

Reinecke, W. G., & McKay, W. L. (1969). *Experiments on water drop breakup behind mach 3 to 12 shocks* (SC-CR-70-6063).

Reinecke, W. G., & Waldman, G. D. (1970). *A study of drop breakup behind strong shocks with applications to flight* (AVSD-0110-70-RR).

Settles, G. S. (2001). *Schlieren and shadowgraph techniques* (First ed.). Springer-Verlag Berlin Heidelberg.

Shimasaki, S., & Taniguchi, S. (2011). Formation of uniformly sized metal droplets from a capillary jet by electromagnetic force. *Applied Mathematical Modeling*, *35*, 1571-1580.

Theofanous, T. G., & Li, G. J. (2008). On the physics of aerobreakup. *Physics of Fluids*, *20*(5), 052103. doi:

Theofanous, T. G., Li, G. J., Dinh, T. N., & Chang, C.-H. (2007). Aerobreakup in disturbed subsonic and supersonic flow fields. *Journal of Fluid Mechanics*, *193*, 131-170. doi: